

# Rainbows in the QCD phase diagram

J. Maelger,<sup>1,2</sup> U. Reinosa,<sup>1</sup> and J. Serreau<sup>2</sup>

<sup>1</sup>*Centre de Physique Théorique, Ecole Polytechnique,  
CNRS, Université Paris-Saclay, F-91128 Palaiseau, France.*

<sup>2</sup>*Astro-Particule et Cosmologie (APC), CNRS UMR 7164, Université Paris Diderot,  
10, rue Alice Domon et Léonie Duquet, 75205 Paris Cedex 13, France.*

(Dated: March 12, 2019)

We study the phase diagram of strongly interacting matter with light quarks using a recently proposed, small parameter approach to infrared QCD in the Landau gauge. This is based on an expansion with respect to both the inverse number of colors and the Yang-Mills coupling in the presence of a Curci-Ferrari mass term. At leading order, this leads to the well-known rainbow equation for the quark propagator with a massive gluon propagator. We solve the latter at nonzero temperature and chemical potential using a simple semi-analytic approximation known to capture the essence of chiral symmetry breaking in the vacuum. In the chiral limit, we find a tricritical point which becomes a critical endpoint in the presence of a nonzero bare quark mass, in agreement with the results of nonperturbative functional methods and model calculations. This supports the idea that the present approach allows for a systematic study of the QCD phase diagram in a controlled expansion scheme.

Hadronic matter is expected to present a rich phase structure when submitted to sufficiently high energy and baryonic densities, large magnetic fields, etc., as encountered in various environments such as the early universe, ultradense astrophysical objects, or relativistic heavy ion collisions in the laboratory [1–3]. Unravelling the phase diagram of quantum chromodynamics (QCD) at nonzero temperature  $T$  and baryonic chemical potential  $\mu_B$  is a major challenge both experimentally and theoretically. At vanishing chemical potential, first principle lattice simulations unambiguously demonstrate a smooth crossover from a mostly confined to a mostly deconfined phase, accompanied by a restoration of chiral symmetry [4, 5]. The crossover region sharpens for increasing quark masses and turns in a second order phase transition for critical values of the quarks masses, above which the transition is first order. The same is expected to happen with the chiral transition in the opposite limit of decreasing quark masses: the transition turns first order below a critical value of the quark masses. Although not firmly established by lattice calculations yet [6], this is the expected behavior of a theory with at least three light quark flavors. The situation with two light quarks is more subtle due to the possible role of the axial anomaly [7].

The situation is even less clear at  $\mu_B \neq 0$  in the low quark mass region (including the physical point), where standard Monte Carlo algorithms are plagued by the infamous sign problem [8]. The typical expectation is that of a line of first order chiral transition at low temperatures ending at a critical point [9]. Firmly establishing the existence of the latter and studying its possible experimental signatures has been the topic of intense theoretical work [10–16] and is among the major physics goals of various present and upcoming experiments [17–20]. Methods to circumvent the sign problem on the lattice have been devised but remain, so far, limited to  $\mu_B/T \lesssim 1$ , and no critical endpoint has been firmly established [21].

To go beyond, a fruitful proposal has been to supplement lattice results for the quenched gluon dynamics with explicit quark contributions by means of nonperturbative functional methods [22–24]. Existing works neglect the mesonic degrees of freedom—although baryons have been included [24]—and find a critical endpoint at a relatively large  $\mu_B/T \gtrsim 3$ . A complementary approach uses phenomenological, Nambu-Jona-Lasinio or quark-meson models with various degrees of sophistication [25–29]. These typically predict a critical endpoint at relatively large  $\mu_B/T$ , whose precise location, however, varies significantly from one study to another. One common weakness of such approaches is that the employed approximations lack a systematic ordering principle. One typically explores the whole phase diagram with truncations adjusted against lattice data at  $\mu_B = 0$ , far from the region where a critical point is found.

In the present Letter, we study this question using a semi-perturbative approach to the infrared dynamics of QCD based on a simple massive extension of the Faddeev-Popov (FP) Lagrangian in the Landau gauge, known as the Curci-Ferrari (CF) model [30, 31]. In this context, the gluon mass term is motivated both by the results of lattice simulations [32] and by the necessity to modify the FP Lagrangian in the infrared due to Gribov ambiguities [33]. The CF model is the simplest renormalizable deformation of the FP Lagrangian and remains under perturbative control down to the deep infrared: The gluon mass screens the standard perturbative Landau pole and the (running) gauge coupling remains moderate at all scales [31, 34], as observed in lattice simulations. A series of recent studies has shown that the perturbative Curci-Ferrari model gives an accurate description of the phase structure of pure Yang-Mills theories and of QCD with heavy quarks [35–37]. The case of light quarks is more delicate because, unlike the couplings in the pure gauge sector, the quark-gluon coupling becomes signif-

icant in the infrared [38]. A systematic approximation scheme, nonperturbative in the quark-gluon vertex, has been proposed in Ref. [39], based on a double expansion in powers of the pure gauge coupling and of the inverse number of colors  $1/N_c$ . At leading order, this successfully describes the dynamics of chiral symmetry breaking in the vacuum. The purpose of the present work is to extend this approach to nonzero temperature and chemical potential and to study the predictions for the phase diagram at leading order in this expansion scheme.

For simplicity, we study a theory with  $N_f$  degenerate quarks. We focus on the quark propagator, more precisely on the quark mass function, which plays the role of an order parameter for the chiral transition. As detailed in [39], at leading order in the double expansion, the quark propagator resums the infinite series of so-called rainbow diagrams [40]. At nonzero temperature  $T$  and quark chemical potential  $\mu = \mu_B/3$ , the rainbow equation for the (Euclidean) quark propagator  $S$  reads

$$S^{-1}(P) = M_0 - (i\omega - \mu)\gamma_0 - \vec{p} \cdot \vec{\gamma} + 4g_0^2 \int_Q^T \gamma_\mu S(Q) \gamma_\nu G_{\mu\nu}(P - Q), \quad (1)$$

where  $Q = (\omega_n, \vec{q})$  and  $P = (\omega, \vec{p})$ , with  $\omega_n = (2n+1)\pi T$  and  $\omega$  fermionic Matsubara frequencies, and where  $\gamma_\mu$  are the Euclidean Dirac matrices, with  $\{\gamma_\mu, \gamma_\nu\} = 2\delta_{\mu\nu}$ . We use the notation  $\int_Q^T f(Q) \equiv T \sum_{n \in \mathbb{Z}} \int \frac{d^3q}{(2\pi)^3} f(\omega_n, \vec{q})$ , where the three-dimensional momentum integral is to be understood with an ultraviolet cut-off. The tree-level gluon propagator is  $G_{\mu\nu}(K) = P_{\mu\nu}^\perp(K)/(K^2 + m^2)$ , with  $P_{\mu\nu}^\perp(K) = \delta_{\mu\nu} - K_\mu K_\nu / K^2$  the transverse projector and  $m$  the gluon mass. Finally,  $M_0$  and  $g_0$  denote the bare quark mass and quark-gluon coupling, respectively.

Parity and rotation invariance imply that the inverse quark propagator can be decomposed as

$$S^{-1}(P) = B - iA_0\gamma_0 - iA_v\vec{p} \cdot \vec{\gamma} - iC\gamma_0\vec{p} \cdot \vec{\gamma}, \quad (2)$$

where the functions  $B$ ,  $A_0$ ,  $A_v$ , and  $C$  only depend on  $\omega$  and  $p = |\vec{p}|$ . An unbroken chiral symmetry implies  $B = C = 0$ . The rainbow equation (1) yields a system of integral equations for the four scalar components in Eq. (2). Here, we focus on the mass function  $B$ —the most relevant ingredient for the description of chiral symmetry breaking—and we set the other functions to their tree-level values,  $A_0 = \omega + i\mu$ ,  $A_v = 1$ , and  $C = 0$ .

With this ansatz, the rainbow equation for the quark mass function  $B$  reads

$$B(P) = M_0 + 4g_0^2 \int_Q^T \frac{B(Q)}{Q_\mu^2 + B^2(Q)} \frac{1}{(P - Q)^2 + m^2}, \quad (3)$$

where we have defined  $Q_\mu \equiv (\omega_n + i\mu, \vec{q})$ . From its definition, we have  $B^*(\omega, p) = B(-\omega, p)$ . This equation can be solved numerically, *e.g.*, by successive iterations. To keep the discussion as simple as possible, we shall further simplify Eq. (3) by using a scheme called localization

[41], which amounts to replacing the mass function by a constant, typically, its value at zero momentum. This is known to correctly capture the phenomenology of chiral symmetry breaking in the vacuum. However, the implementation of this scheme at nonzero temperature and chemical potential is not completely straightforward because the fermionic Matsubara frequencies never vanish. One possible choice is to replace  $B(Q) \rightarrow B(\pm\omega_1, 0)$ , with  $\omega_1 = \pi T$  the lowest Matsubara frequency. However, in that case, one has to treat the problem in the complex plane because  $B(\pm\omega_1, 0)$  is not real. Here, we make a simpler choice in order to minimize the degree of complication of the problem. We consider the retarded component of the quark mass function, which is directly related to the actual pole mass and which is real at zero frequency and momentum. It can be obtained from the analytic continuation of  $B(Q)$  to the complex frequency plane as  $B_R(q_0, q) = B(-i(q_0 + \mu) + 0^+, q)$ , with  $q_0 \in \mathbb{R}$ . We then localize the rainbow equation for the retarded mass function by replacing  $B_R(q_0, q) \rightarrow B_R(0, 0) \equiv B \in \mathbb{R}$ .

In practice, this amounts to replacing  $B(Q) \rightarrow B$  in (3), perform explicitly the Matsubara sum on the right-hand side (this is important in order to obtain the proper analytic continuation), and evaluate the resulting expression at  $\omega = -i\mu + 0^+$  and  $p = 0$ . We obtain

$$\left(1 - \frac{g_0^2}{\pi^2} [F_{\text{vac}}(B) + F_{\text{th}}(B)]\right) B = M_0, \quad (4)$$

with

$$F_{\text{vac}}(B) = \int_0^\Lambda dq \frac{q^2}{\varepsilon_q^m \varepsilon_q^B (\varepsilon_q^m + \varepsilon_q^B)}, \quad (5)$$

where  $\varepsilon_y^x \equiv \sqrt{x^2 + y^2}$ , and

$$F_{\text{th}}(B) = \frac{2}{B^2 - m^2} \int_0^\infty dq q^2 \left( \frac{n_{\varepsilon_q^m}^{(-)}}{\varepsilon_q^m} + \frac{n_{\varepsilon_q^B - \mu}^{(+)} + n_{\varepsilon_q^B + \mu}^{(+)}}{2\varepsilon_q^B} \right), \quad (6)$$

where  $n_x^{(\pm)} = (e^x \pm 1)^{-1}$  denote the Bose-Einstein and Fermi-Dirac distributions. One price to pay for our choice of localization is the singularity at  $B = m$ , which is regulated, in the retarded self energy through  $B^2 - m^2 \rightarrow B^2 - m^2 + i0^+$ . We ignore this issue and restrict our analysis to cases where  $B < m$ . This is justified both because the physically relevant values in the vacuum fall in this range (see below) and because most of our discussions below concern the vicinity of the symmetric point  $B = 0$ .

Consider first the chiral limit  $M_0 = 0$ . For large enough values of the coupling, Eq. (4) admits nontrivial, symmetry breaking solutions on top of the chirally symmetric solution  $B = 0$ . It is convenient to parametrize the equation in terms of the dynamical mass in the vacuum,  $B_0 \equiv B(T = 0, \mu = 0)$ , given by

$$F_{\text{vac}}(B_0) = \pi^2/g_0^2, \quad (7)$$

where we see that symmetry-breaking solutions exist only

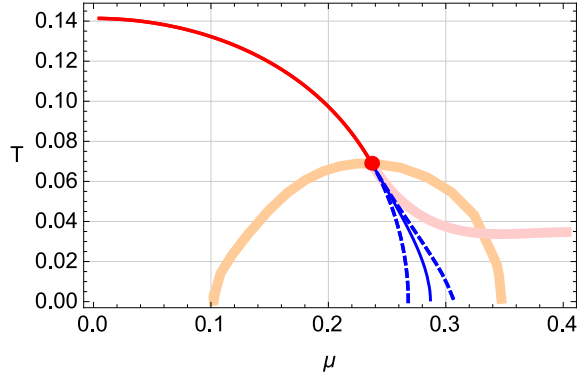


FIG. 1. Phase diagram in the chiral limit (all scales in GeV), with  $B_0 = 0.3$  GeV and  $m = 0.5$  GeV. The line of second-order transitions (solid red) turns into a line of first-order transitions (solid blue) at the tricritical point (red dot). The dashed curves are the corresponding spinodal lines. The orange line shows the location of the tricritical point as a function of the gluon mass (see text). Away from the chiral limit, the tricritical point turns into a critical endpoint, whose position follows the pink line as the bare quark mass is increased.

if  $g_0^2 > \pi^2/F_{\text{vac}}(0)$ . We use Eq. (7) to trade the bare quark-gluon coupling  $g_0$  for the (ultraviolet finite) quark mass  $B_0$ . The rainbow equation rewrites as

$$2BR(B^2) \equiv B[F_{\text{vac}}(B_0) - F_{\text{vac}}(B) - F_{\text{th}}(B)] = 0, \quad (8)$$

where the cut-off can now be sent to infinity:

$$F_{\text{vac}}(B_0) - F_{\text{vac}}(B) = \frac{B^2 \ln(B/m)}{2(B^2 - m^2)} - \frac{B_0^2 \ln(B_0/m)}{2(B_0^2 - m^2)}. \quad (9)$$

It is useful to interpret Eq. (8) as deriving from a chirally symmetric potential  $W(B^2)$ , with  $\partial_B W(B^2) = 2BR(B^2)$ , that is  $W'(B^2) = R(B^2)$ . The absolute minima of  $W(B^2)$  then determine the state of the system. At  $\mu = 0$ , one easily checks that the nontrivial minimum  $B_0$  in the vacuum decreases with increasing temperature and continuously reaches  $B = 0$  at a critical temperature. This extends in a critical line of second-order phase transitions  $T_c(\mu)$  in the  $(\mu, T)$  plane, defined by the condition  $W'(0) = 0$ , as shown in Fig. 1. Depending on the parameters, this critical line can turn in a line of first-order transitions at a tricritical point, defined by the conditions  $\partial_B^{(2n)} W(B^2)|_{B=0} = 0$  for  $n = 1, 2$  or, equivalently,

$$W'(0) = W''(0) = 0. \quad (10)$$

The first-order line is then determined from

$$W'(B_{\text{min}}^2) = W(B_{\text{min}}^2) - W(0) = 0, \quad (11)$$

where  $B_{\text{min}}$  is the nontrivial minimum at the transition. The associated lower and upper spinodals are respec-

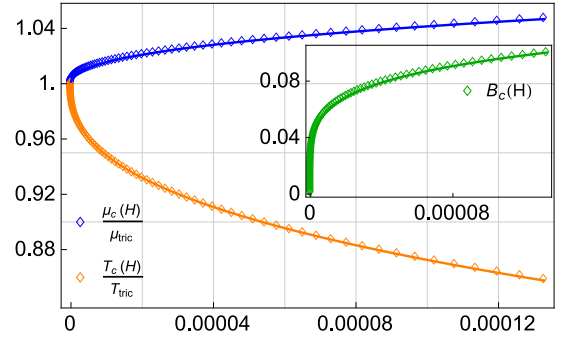


FIG. 2. The approach of the critical quantities  $\mu_c(H)$ ,  $T_c(H)$ , and  $B_c(H)$  to the chiral limit shows mean field tricritical scaling with mean field exponents. The solid lines are power law fits of the form  $A_c(H) - A_{\text{tric}} \propto H^{\omega_A}$  for  $A = \mu, T, B$  with mean field exponents  $\omega_T = \omega_\mu = 2/5$  and  $\omega_B = 1/5$ .

tively defined by

$$W'(0) = 0 \quad \text{and} \quad W'(B_{\text{sp}}^2) = W''(B_{\text{sp}}^2) = 0, \quad (12)$$

with  $B_{\text{sp}}$  the location of the nontrivial metastable state at the upper spinodal. The two spinodals flank the first order line and merge at the tricritical point, beyond which the lower spinodal becomes the critical line. The equation governing the the critical and lower spinodal lines is easily obtained as

$$\mu^2(T) = m^2 \frac{B_0^2 \ln(B_0/m)}{B_0^2 - m^2} - 4 \int_0^\infty dq q^2 \frac{n_{\varepsilon_q}^{(-)}}{\varepsilon_q^m} - \frac{\pi^2}{3} T^2, \quad (13)$$

which is a strictly concave line. For low enough temperatures  $T/m \ll 1$ , the gluon contribution (second term) in Eq. (13) is negligible and one approximates

$$\mu^2(T) \approx m^2 \frac{B_0^2 \ln(B_0/m)}{B_0^2 - m^2} - \frac{\pi^2}{3} T^2. \quad (14)$$

This is similar the result obtained in the quark-meson model with a large- $N_f$  approximation [25].

There is an ambiguity in the definition of the potential  $W(B^2)$  since neither the solutions of Eq. (8) nor their convexity are altered by the replacement  $W'(B^2) \rightarrow f_+(B^2)R(B^2)$  with  $f_+(B^2)$  a differentiable and strictly positive function. Interestingly, because the conditions (10) and (12) only involve  $W'$  and its derivatives, they are, in fact, independent of the function  $f_+$  and so are, thus, the spinodal lines, the line of second-order transition, and, of course, the tricritical point where these lines meet. Only the line of first-order transition explicitly depends on  $f_+$  through the second condition in Eq. (11). However, it always lies in between the two spinodals.

In Fig. 1, we show our results for the phase diagram in the chiral limit. We use the typical values  $m = 500$  MeV and  $B_0 = 300$  MeV, motivated by the study of dynamical chiral symmetry breaking in the Curci-Ferrari model

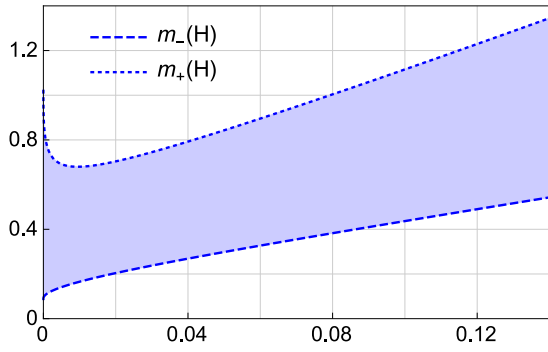


FIG. 3. Allowed values of the gluon mass  $m$  for a (tri)critical point to exist as a function of  $H$  (blue area). All in GeV.

in the vacuum [39]. We find a tricritical point located at  $(\mu, T) \approx (237 \text{ MeV}, 69 \text{ MeV})$ . The transition at zero chemical potential occurs at  $T_c(\mu = 0) \approx 141 \text{ MeV}$  and the two spinodals meet the  $T = 0$  axis for  $\mu \approx 268 \text{ MeV}$ , and  $\mu \approx 305 \text{ MeV}$ , respectively. This gives an estimate of the first-order transition line at most at the 10% level, independently of the function  $f_+$  (the estimate improves as one approaches the tricritical point). For the choice  $f_+ = 1$ , the  $T = 0$  transition point is at  $\mu \approx 287 \text{ MeV}$ .

In fact, Eq. (8) greatly simplifies at  $T = 0$ , where

$$F_{\text{th}}(B) = \frac{B^2/2}{B^2 - m^2} \left[ \frac{\mu}{B} \sqrt{\frac{\mu^2}{B^2} - 1} - \cosh^{-1} \left( \frac{\mu}{B} \right) \right], \quad (15)$$

if  $\mu \geq B$  and  $F_{\text{th}}(B) = 0$  otherwise. In particular, we see that the value of the order parameter below the transition point is independent of  $\mu$ ,  $B(T = 0, \mu) = B_0$ , until it jumps to  $B = 0$  in the symmetric phase. This is known as the Silver Blaze property [42, 43]. Also, using Eqs. (9) and (15), we can determine the values of the gluon mass for which there exists a tricritical point. The latter reaches the  $T = 0$  axis for some values of the ratio  $x = m/B_0$ . Defining  $u = (\ln x^2)/(x^2 - 1)$ , we get the condition  $u = 1 + \ln(2u)$ , which has two solutions in  $\mathbb{R}^+$ ,  $u_{\pm} = u(x_{\pm})$ , with  $x_+ x_- = 1$ . One finds  $x_- = \sqrt{u_+/u_-} \approx 0.294$  and  $x_+ \approx 3.398$ . The corresponding values of  $y = \mu/B_0$  are given by Eq. (13) at  $T = 0$ ,  $y^2 = x^2 u/2$ , yielding  $y_- = \sqrt{u_+/2} \approx 0.340$  and  $y_+ = y_-/x_- \approx 1.157$ . There exists a tricritical point iff  $x \in [x_-, x_+]$  as shown in Fig. 1.

Let us now move away from the chiral limit. Equation (8) now reads  $2BR(B^2) = H$ , with  $H = \pi^2 M_0/g_0^2$  the symmetry breaking parameter. For  $H \neq 0$ , the second-order transitions turn into crossovers and the tricritical point becomes a critical endpoint terminating a first-order line. Writing the potential  $V(B) = -HB + W(B^2)$ , the conditions for a critical point are

$$V'(B_c) = V''(B_c) = V'''(B_c) = 0, \quad (16)$$

from which one extracts  $B_c$ ,  $T_c$ , and  $\mu_c$  for each  $H$ . To this aim, it is convenient to vary  $B$ , determine  $T_c(B)$  and  $\mu_c(B)$  from the last two conditions in Eq. (16)—that do not involve  $H$ —and then deduce  $H(B)$  from the first condition. Inverting this relation, one then accesses  $T_c(H)$  and  $\mu_c(H)$ . In particular, we find that the approach to tricriticality is governed by mean field exponents; see Fig. 2. This is expected because the potential is regular around  $B = 0$ . The trajectory of the critical endpoint in the phase diagram, shown in Fig. 1, is similar to that observed in Ref. [12]. Finally, Fig. 3 shows the interval  $[x_-(H), x_+(H)]$  compatible with a critical point.

To conclude, we have computed the phase diagram of QCD with light quarks in the context of a first-principle inspired approach to infrared QCD, the Curci-Ferrari model, using the double expansion in the pure gauge coupling and in  $1/N_c$  proposed in Ref. [39]. For the parameters used here, the leading-order results agree well with those of effective quark-meson models when the chiral anomaly is neglected [25, 29]. Although subleading in  $1/N_c$ , the latter and meson fluctuations are important to correctly determine the phase structure in the Columbia plot [7, 29, 44]. In principle, they can be systematically included at next-to-leading order in the present expansion scheme.

We also mention that similar rainbow equations have already been considered in great detail to study the phase diagram in the context of nonperturbative functional approaches [12, 22]. Not too surprisingly, our results agree qualitatively with those (the main differences may be attributed to the different treatments of the gluon sector). However, the key point of the present work is to systematically justify the employed approximation on the basis of identified small parameters in QCD.

Although we used here the simple version (4) of the complete rainbow equation (1), we expect, inspired by the vacuum case, that our main results are robust. One interesting point that deserves particular attention is the observation that the existence of a (tri)critical point seems to require a nonzero gluon mass. It is interesting to investigate to what extent this is an artifact of the localization procedure used here, for instance, by devising alternative localization schemes. Another, obvious extension of the present work will be to solve Eq. (3) for the momentum-dependent mass function  $B$  and, further, to include the other scalar functions  $A_0$ ,  $A_v$ , and  $C$  in Eq. (1), as partially done in Refs. [22, 23].

Yet another interesting direction of investigation is to include the order parameter of the deconfinement transition, the Polyakov loop, in the spirit of Refs. [35–37], which would allow one to study the interplay between the chiral and deconfinement phase transition across the Columbia plot [26, 45, 46].

We thank Zs. Szép for interesting discussions and helpful remarks concerning the manuscript.



- 
- [1] K. Fukushima and T. Hatsuda, Rept. Prog. Phys. **74** (2011) 014001.
- [2] S. Weissenborn, I. Sagert, G. Pagliara, M. Hempel and J. Schaffner-Bielich, Astrophys. J. **740** (2011) L14.
- [3] S. Borsányi *et al.*, Nature (London) **539** (2016) 69.
- [4] Y. Aoki, Z. Fodor, S. D. Katz and K. K. Szabo, Phys. Lett. B **643** (2006) 46.
- [5] A. Bazavov *et al.*, Phys. Rev. D **85** (2012) 054503.
- [6] M. D’Elia, Nucl. Phys. A **982** (2019) 99.
- [7] R. D. Pisarski and F. Wilczek, Phys. Rev. D **29** (1984) 338.
- [8] P. de Forcrand, PoS LAT **2009** (2009) 010;
- [9] M. A. Stephanov, Prog. Theor. Phys. Suppl. **153** (2004) 139 [Int. J. Mod. Phys. A **20** (2005) 4387].
- [10] B. Mohanty and J. Serreau, Phys. Rept. **414** (2005) 263.
- [11] M. A. Stephanov, Phys. Rev. Lett. **102** (2009) 032301.
- [12] Y. Hatta and T. Ikeda, Phys. Rev. D **67** (2003) 014028.
- [13] C. D. Roberts and S. M. Schmidt, Prog. Part. Nucl. Phys. **45** (2000) S1.
- [14] C. S. Fischer, arXiv:1810.12938 [hep-ph].
- [15] K. Fukushima and C. Sasaki, Prog. Part. Nucl. Phys. **72** (2013) 99.
- [16] H. T. Ding, F. Karsch and S. Mukherjee, Int. J. Mod. Phys. E **24** (2015) 1530007.
- [17] B. Mohanty (STAR Collaboration), J. Phys. G **38** (2011) 124023.
- [18] P. Senger, Eur. Phys. J. A **52** (2016) 217.
- [19] T. Ablyazimov *et al.* [CBM Collaboration], Eur. Phys. J. A **53** (2017) 60.
- [20] T. Sakaguchi [J-PARC-HI Collaboration], Nucl. Phys. A **967** (2017) 896.
- [21] Z. Fodor *et al.*, arXiv:1807.09862 [hep-lat].
- [22] C. S. Fischer and J. Luecker, Phys. Lett. B **718** (2013) 1036.
- [23] C. S. Fischer, L. Fister, J. Luecker and J. M. Pawłowski, Phys. Lett. B **732** (2014) 273.
- [24] G. Eichmann, C. S. Fischer and C. A. Welzbacher, Phys. Rev. D **93** (2016) 034013.
- [25] A. Jakovác, A. Patkós, Z. Szép and P. Szépfalusy, Phys. Lett. B **582** (2004) 179; Acta Phys. Hung. A **22** (2005) 355.
- [26] B. J. Schaefer, J. M. Pawłowski and J. Wambach, Phys. Rev. D **76** (2007) 074023.
- [27] K. Fukushima, Phys. Rev. D **77** (2008) 114028 Erratum: [Phys. Rev. D **78** (2008) 039902].
- [28] T. K. Herbst, J. M. Pawłowski and B. J. Schaefer, Phys. Lett. B **696** (2011) 58; Phys. Rev. D **88** (2013) 014007.
- [29] S. Resch, F. Rennecke and B. J. Schaefer, arXiv:1712.07961 [hep-ph].
- [30] G. Curci and R. Ferrari, Nuovo Cim. A **32** (1976) 151.
- [31] M. Tissier and N. Wschebor, Phys. Rev. D **82** (2010) 101701; Phys. Rev. D **84** (2011) 045018.
- [32] I. L. Bogolubsky, E. M. Ilgenfritz, M. Müller-Preussker and A. Sternbeck, Phys. Lett. B **676** (2009) 69.
- [33] J. Serreau and M. Tissier, Phys. Lett. B **712** (2012) 97.
- [34] U. Reinosa, J. Serreau, M. Tissier and N. Wschebor, Phys. Rev. D **96** (2017) 014005.
- [35] U. Reinosa, J. Serreau, M. Tissier and N. Wschebor, Phys. Lett. B **742** (2015) 61; Phys. Rev. D **91** (2015) 045035; Phys. Rev. D **93** (2016) 105002.
- [36] U. Reinosa, J. Serreau and M. Tissier, Phys. Rev. D **92** (2015) 025021.
- [37] J. Maelger, U. Reinosa and J. Serreau, Phys. Rev. D **97** (2018) 074027. Phys. Rev. D **98** (2018) 094020.
- [38] J. I. Skullerud, P. O. Bowman, A. Kizilersu, D. B. Leinweber and A. G. Williams, JHEP **0304** (2003) 047.
- [39] M. Peláez, U. Reinosa, J. Serreau, M. Tissier and N. Wschebor, Phys. Rev. D **96** (2017) 114011.
- [40] G. ’t Hooft, Nucl. Phys. B **75** (1974) 461.
- [41] G. Markó, U. Reinosa and Z. Szép, Phys. Rev. D **92** (2015) 125035.
- [42] T. D. Cohen, Phys. Rev. Lett. **91** (2003) 222001.
- [43] G. Markó, U. Reinosa and Z. Szép, Phys. Rev. D **90** (2014) 125021.
- [44] J. T. Lenaghan, Phys. Rev. D **63** (2001) 037901.
- [45] K. Fukushima, Phys. Lett. B **591** (2004) 277.
- [46] A. S. Folkestad and J. O. Andersen, arXiv:1810.10573 [hep-ph].